

## EFFECT OF PARTICLES IN A TURBULENT GAS-PARTICLE FLOW WITHIN A 90° BEND

K. MOHANARANGAM<sup>1,2</sup>, W. YANG<sup>2</sup>, H. J. ZHANG<sup>2,3</sup> and J. Y. TU<sup>1</sup>

<sup>1</sup> School of Aerospace, Mechanical and Manufacturing Engineering, RMIT University, Victoria 3083, AUSTRALIA

<sup>2</sup> CSIRO Minerals, Clayton, Victoria 3169, AUSTRALIA

<sup>3</sup> China Jiliang University, Hangzhou, Zhejiang, P.R. CHINA

jiyuan.tu@rmit.edu.au

### ABSTRACT

Simultaneous measurements of both the carrier gas phase and the dispersed particulate phase were carried out inside a curved 90° duct bend. These measurements were undertaken in order to investigate the effects of dilute turbulent particulate flows on the gas phase and vice versa. The investigations were carried out experimentally in the Advanced Laser Diagnostic Laboratory at CSIRO Division of Minerals using 2D Phase Doppler Anemometry (PDA). The main objective of the current study is to decipher the effect of streamwise and transverse velocities of the particles on the gas phase. This study has also been carried out with the view of obtaining robust experimental data for developing (and validating) accurate CFD models. Glass spheres with mean diameter of 77µm were used to represent the solid phase, while the carrier gas phase has a working Reynolds number of  $Re=1.0 \times 10^5$  (bulk velocity  $U_o=10\text{ms}^{-1}$ ). The gas phase results were analysed as both clean gas (without any particles) and unclean gas (with particles). The unclean gas results were separated from the particles based on their size in the post-processing step of the laser data. It is observed that the streamwise and the transverse velocities of the unclean gas phase 'lagged' behind the clean gas velocities from the mid section of the duct towards the inner bend wall. Also, the same feature is observed along the vertical duct past the 90° bend. This phenomenon is mainly attributed to the effect of the particles drag on the continuous gas phase.

### NOMENCLATURE

$D$  duct height, m  
 $U_o$  bulk velocity,  $\text{ms}^{-1}$   
 $U$  mean streamwise velocity,  $\text{ms}^{-1}$   
 $V$  mean transverse velocity,  $\text{ms}^{-1}$   
 $Re$  Reynolds number  
 $r$  distance from the outer wall, m  
 $r^*$  dimensionless distance from the outer wall  
 $St$  Stokes number  
 $t_p$  particle relaxation time, s  
 $t_s$  time characteristic of fluid motion, s  
 $\theta$  angle along the bend, degree  
 $x$

### INTRODUCTION

Dilute gas-particle flows are encountered in a range of naturally and artificially occurring flows. Industrially occurring gas-particle flows have been a subject of interest to scientists and engineers for decades as they have widespread applications in chemical and mechanical processing industries. The behaviour of the particles

amidst the gas phase is a deterministic factor in a lot of design engineering problems, as the addition of another phase (particles) causes a well marked change in the way the carrier phase behaves.

Gas-solid flows have many applications in chemical, food processing, pharmaceutical, cement and power industries. In many of these industries the gas and the solid are conveyed in large ducts with velocities ranging from 10-25 $\text{ms}^{-1}$  and with a wide range of solids loading ratios. 90° bends are often used to change the direction of these two phase flows, and to save space given the complexity of these operating plants. Flows within curved bends are quite complex and are characterized by a stress field with stabilizing effects near to the inner-radius and destabilizing effects close to the outer radius (Humphrey et al, 1981). In fact they are well known to create flow problems, even in single phase flow (Bilirgern & Levy, 2001). Addition of another phase within these bends are set to changes the entire flow features, leading to the formation of a 'so called' third phase due to the roping characteristics of the particles (Yilmaz & Levy, 2001).

Non-intrusive two-phase laser studies in curved ducts were first carried out by Kliafas and Holt (1987). Detailed LDV studies were carried out by them in a square sectioned 90° vertical to horizontal duct bend. Simultaneous measurements of the mean streamwise and radial velocities and the associated Reynolds stresses were made at 15 planes, two Reynolds numbers and two particle sizes. This was done in order to directly benefit the large scale coal gasification plants, where these bends are used quite often. However, both the phases were measured separately owing to a dilute particle concentration in the flow. The pneumatic conveying through various pipe elements and configurations was also studied in detail by Huber and Sommerfeld (1994) using the PDA technique. They concluded that besides the non-uniformity in the particle concentration, a bend causes considerable particle segregation, which again is more pronounced for lower superficial gas velocity and higher particle loading. As the solids and the air flow past the bend, the particles tend to locally concentrate within the elbow, mostly within the outer section of the elbow bend. This feature is caused by the inertial and the centrifugal forces acting on the particles once they flow past the bend giving rise to a feature called 'particle roping'. This feature results in the velocity of the particles to be reduced by one half of the mean gas velocity along with relatively high particle concentration (Yilmaz & Levy, 2001). In coal fired power plants the roping phenomenon is responsible for flow

control and measurement problems and it is widely attributed to be a limiting factor in the ability to reduce  $\text{NO}_x$  and combustion efficiency (Yilmaz & Levy, 1998).

Yang & Kuan (2006) carried out experiments of dilute turbulent particulate flows inside a square ducted  $90^\circ$  bend. Their main aim was to investigate the presence of so called ‘particle ropes’ at low mass loadings (i.e., solids mass loading  $<0.1$ ) which is quite typical in dilute mill duct system. They concluded that the high turbulence intensity in the early part of the bend is due to the frequent particle-wall collisions, which in turn was due to the presence of a high particle concentration region next to the outer wall. This led to the formation of ‘particle rope’ structure.

Numerical simulations using a Lagrangian particle tracking approach were carried out by Kuan et al. (2007) to validate the experimental data of Yang and Kuan (2006). Numerical simulations were also carried out by Tu and Fletcher (1995) in a  $90^\circ$  bend using an Eulerian two-fluid model. In their study mean streamwise velocities of clean gas and particles were compared against the experimental data of Kliafas and Holt (1987). Streamwise fluctuating velocities of clean gas were also compared against the experimental data using standard and RNG based  $k-\epsilon$  model. Later the same model was extended to predict the particle fluctuation by Mohanarangam et al. (2007).

In all of the above mentioned numerical studies obtaining accurate predictions from the inner to the middle section of the bend radius was rather cumbersome. This is mainly due to the preferential concentration of the particles at the outer bend. In fact most of the experiments were carried out by measuring only the gas phase or only the particulate phase. The main drawback of this procedure is the effect or changes the particles impart on the gas phase is totally lost, especially near the inner wall of the bend where the particles are least present. In order to alleviate this problem, the researchers in this current paper measured simultaneously the gas as well as the particle. An accurate CFD model could then be developed to replicate the measured ‘unclean’ gas velocities, which currently most of the numerical models fail to capture.

In this paper similar experiments to that of Yang & Kuan (2006) were carried out, with a higher mass loading but still less than 0.1. This was done deliberately in order to establish a healthy two-way coupling between the continuous and the dispersed phases. The current experiments were carried out specifically to study the effects of the particles on the streamwise and transverse gas velocities inside the curved  $90^\circ$  bend duct. The gas velocity profiles across the vertical centre plane of the duct at various locations were measured with (unclean gas) and without (clean gas) the presence of the dispersed particulate phase by using Phase Doppler Anemometry (PDA).

## EXPERIMENTAL APPARATUS

As described in Yang & Kuan (2006), all experiments were carried out in an open-circuit suction wind tunnel system. The  $150 \times 150$  ( $\text{mm}^2$ ) square test section was constructed using 10mm thick Perspex, and consisted of a

3.5m-long horizontal straight duct, a curved  $90^\circ$  bend with a radius ratio of 1.5, and a 1.8m-long vertical straight duct.

Figure 1 shows the geometry of the curved  $90^\circ$  bend, where simultaneous two-phase velocity measurements were taken at  $15^\circ$  interval within the bend, followed by several sections along the vertical duct. However, experimental results in only a few sections are reported in this paper for brevity.

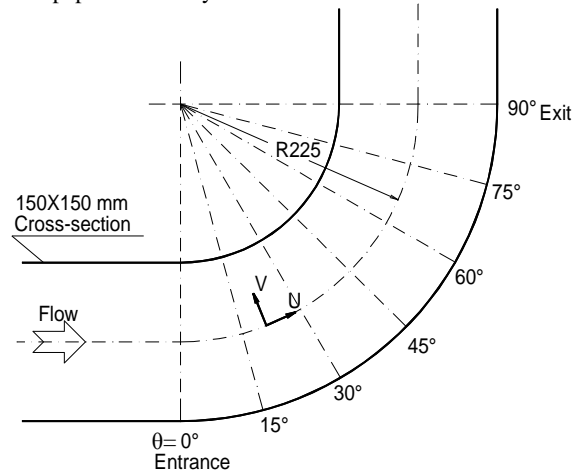


**Figure 1.** Geometry of curved  $90^\circ$  bend test section

All results presented in this paper were obtained with the bulk gas velocity of  $10\text{ms}^{-1}$ , and the turbulence intensity at the centre of duct cross section  $10D$  upstream of the  $90^\circ$  bend was at 1%. The Reynolds number ( $Re$ ), based on the bulk velocity, hydraulic diameter of the squared cross section and kinematic viscosity of air was  $1.0 \times 10^5$ . The solid particles used in the study were glass spheres with an average diameter of  $77\mu\text{m}$ . A twin-screw gravity particle feeder was utilised to inject the solid particles into the wind tunnel system at a constant flow rate. The seeding particles for the air flow was a fine mist of sugar particles generated by a TSI six-jet Atomizer from a 5% sugar solution.

## PDA TECHNIQUE AND UNCERTAINTY

Phase Doppler Anemometry is an extension of Laser Doppler Anemometry (LDA) and can be used to determine not only the particle velocity which is proportional to the Doppler shift frequency of the scattered light, but also its size based on the fact that the phase shift of the Doppler bursts between two or more photomultipliers is proportional to the particle diameter (Durst & Zare, 1975).

In this investigation, a TSI-Aerometrics 2D LDA/PDA system was utilised to obtain velocity and particle size measurements. This system incorporates a 5W Ar-Ion laser together with a fibre optic system including a transmitting probe of focal length 250mm and a receiving probe with a front lens of focal length 500mm. The system is capable of measuring two velocity components and the particle size simultaneously. For the particle size measurement, an optimum collection angle between the centrelines of the transmitting and receiving probes must be set depending on the refractive indices of the particles and the medium, as well as the choice of the PDA operation mode between reflection and refraction. For the sugar mist seeding particle and the glass beads used in the

experiments, light refracted through the particle in the forward scatter region produces the highest sizing sensitivity, therefore the arrangement of a typical collection angle of  $30^\circ$  for forward scatter in the refraction mode was used in the particle size measurements. Moreover, for the current optical arrangement the measurable particle diameter range was between  $0.5\mu\text{m}$  and  $118\mu\text{m}$ , which is sufficient for the simultaneous measurement of the gas phase seeding particles and the dispersed phase particles.

During the experimental measurements, the mean velocities and sizes of the “clean” gas phase were firstly obtained without the presence of the dispersed particles, and then simultaneous measurements of the “unclean” gas phase and the dispersed particulate phase were performed. By the reference of the size measurements of the “clean” gas phase, the velocity information of the “unclean” gas phase was separated from the simultaneous measurements of both phases at each measuring point. In order to obtain a reasonable statistical average velocity measurement, a minimum validated sample size of 5000 was set for each measuring point.

There are several sources of errors involved using the PDA technique for the simultaneous two-phase measurement. The typical hardware and optical alignment errors of the current PDA system were estimated as 2% for the velocity measurements and 4% for the particle size measurements. Another common error using the PDA technique arises from the cross-talk between the two phases in which the gas seeding particles and the dispersed particles may be incorrectly identified. Moreover, the variable sampling size and particle concentration between different measurement locations may cause some errors. As a consequence, the total uncertainty estimates for the current study were 4% for the velocity measurements and 8% for the size measurements respectively.

## RESULTS AND DISCUSSION

Time-averaged PDA measurements of both the gas (with and without the particles) as well as the particles were obtained in the course of the experiment. The streamwise ( $U$ ) and the transverse ( $V$ ) velocities were measured along the mid-plane of the duct geometry. The above measured quantities are plotted throughout the paper using a non-dimensionalised distance from the outer wall  $r^*$ , which is given by  $r^*=r/D$ . So  $r^*=0.0$  represents the outer wall and  $r^*=1.0$  represents the inner wall of the bend geometry.

Changes caused due to the presence of the particles in the gas streamwise and transverse velocities are analysed. In order to carry out this investigation, the mean streamwise and transverse velocities of the clean gas phase (without the particles) have been plotted with the corresponding unclean gas (with the particles) phase velocities in figures 2-5. The mean particulate phase velocities for the current experimental geometry have already been published by Yang & Kuan (2006), and so have not been plotted here. The clean gas phase velocities are shown by the unfilled circles, while the unclean gas is depicted using the filled circles. These velocities have been normalized against the mean streamwise bulk velocity of  $U_o=10\text{ms}^{-1}$ .

Figure 2 shows the mean streamwise velocity profiles of the gas phase with (unclean) and without (clean) the particles, at six locations through the bend. All the sections except  $15^\circ$  have been shown as there was a meagre difference between bend sections  $15^\circ$  and  $30^\circ$ . It is seen that the velocity at the entry of the bend ( $0^\circ$ ) is already affected by the presence of the bend; this can be easily seen as the flow tries to accelerate with a higher velocity near the inner wall of the bend, setting up a velocity gradient along the transverse section of the duct. A steady acceleration of the flow is seen for both the gas states along the inner wall of the experimental geometry. The maximum streamwise velocity occurs close to the inner wall at the  $45^\circ$  section where  $r^*\approx 0.9$ . It can be seen all along the bend geometry, the gas at the inner wall travels at a higher velocity in comparison to the outer wall. At section  $\theta=0^\circ$  it is observed that there is little or no increase in the mean gas velocities for the unclean gas for  $r^*<0.5$ . However, for  $r^*>0.5$ , the unclean gas velocities lag behind the clean gas velocities. The same phenomenon is also observed for  $\theta=30^\circ$ . As  $r^*$  increases the unclean gas shows an increase in mean velocity followed by a small region of no change and then a significant decrease. At  $\theta=45^\circ$  and  $60^\circ$  this difference is felt even sooner, starting from  $r^*\approx 0.4$  radially. At  $\theta=60^\circ$  for a small section near the inner wall the unclean velocities seem to decrease in magnitude and fall in line with the clean gas velocities. This feature is more pronounced for sections  $\theta=75^\circ$  and  $90^\circ$ . The maximum difference in mean streamwise velocities of  $0.23U_o$  between the clean and the unclean gas occurs at the entrance of the bend near the inner wall. As the flow travels through the bend it loses its momentum near the inner wall, while gaining near the outer wall. This behaviour is attributed to the flow separation at the inner wall, which arises as a result of the adverse pressure gradient found typically in curved bends.

Figure 3 shows the transverse velocity profiles of clean and unclean gas through the bend. Throughout the bend except at the entrance, the transverse velocities are negative i.e., directed towards the outer wall. There is not much change between the clean and unclean gas velocities at the entrance of the bend, with some slight change present near the inner wall. At  $\theta=30^\circ$ , the change is more pronounced between the clean and the unclean gas. The region near the outer wall ( $r^*<0.2$ ) shows little change to the presence of the particles, while as  $r^*$  increases, the change is more distinct, starting from  $r^*=0.4$ . Similar observations can be made at  $\theta=45^\circ$ . The point of change in the unclean gas as  $r^*$  increases is in line with the streamwise gas velocities, showing that the presence of the particles have distinct effect on both the streamwise as well as the transverse velocities. Further into the bend, at sections  $\theta=60^\circ$ ,  $75^\circ$  and  $90^\circ$ , the velocity of the unclean gas shows distinct differences in magnitude from its counterpart clean gas. It is also noted that there is an increase in the tendency of the flow to move towards the outer wall, as  $\theta$  increases, with the maximum difference between the clean and the unclean gas to be  $0.083U_o$ , occurring at the exit of the bend section at  $\theta=90^\circ$ .

Figure 4 shows the mean streamwise velocities of clean and unclean gas along the vertical duct past the bend. Four sections at  $x=0.5D$ ,  $1D$ ,  $3D$  and  $9D$  have been presented. It can be seen at  $x=0.5D$  the velocity magnitude is very uneven. This is because of the separation that has occurred

in the inner section of the bend due to the adverse pressure gradient. This phenomenon is pronounced until  $x=9D$  where the flow has fully recovered from the flow separation and almost assumed a fully developed turbulent channel flow behaviour. At  $x=0.5D$  (just downstream of the bend) the unclean gas lags the clean gas near both walls, while the reverse is true for  $r^*$  between 0.5 and 0.8. The 1D and 3D sections also show a mixed behaviour along the cross-section of the duct. At  $x=9D$ , where flow has fully recovered from the pressure gradients there is a minor change in the magnitude of the unclean gas all along the height of the section, with the unclean gas velocity lagging behind the clean gas.

Figure 5 shows the mean transverse velocities along the vertical duct of the geometry past the bend. The transverse velocities are negative signifying that the flow is still directed towards the outer wall of the bend. It can be clearly seen that the velocities at  $x=0.5D$  and  $1D$  are still recovering from the flow separation. On the local basis it can be seen that the unclean gas flow decreases in magnitude (with less tendency to move towards the outer wall) for  $r^*<0.6$  at  $x=0.5D$ , above which there is mixed behaviour near the inner wall. A similar change for  $x=1D$  occurs at  $r^*<0.5$ . At  $x=3D$  there is an almost uniform and constant change for all  $r^*$ . The same behaviour is also evident at  $x=9D$ ; however the change in velocity magnitude is quite small.

#### *Effect of Particles on the Mean Gas Velocities:*

It can be summarized that the mean flow in the streamwise direction slows down through the bend near the inner wall, while it more or less remains unchanged near the outer wall. The same holds true for the mean transverse velocities. Along the vertical duct past the bend, the streamwise velocities are seen to recover from the pressure gradient effects of the bend with the development of the flow (magnitude) from the inner to the outer wall of the bend as  $x$  increases. The transverse velocities recover as  $x$  increases with the majority of the flow directed towards the outer wall of the bend. Throughout the bend as well as the vertical section after the bend a marked difference can be seen between the clean and the unclean gas. This behaviour of the unclean gas phase velocities can be better explained with definition of Stokes number ( $St$ ). Stokes number is an important dimensionless parameter in defining how particles behave with the gas flow field. It is given by the ratio of the particle relaxation time to a characteristic time of the fluid motion, i.e.,  $St = t_p/t_s$ . This in turn determines the kinetic equilibrium of the particles with the surrounding fluid. In choosing the appropriate fluid time scale  $t_s$ , the inlet height of the duct is taken as the length scale, which is also the span-wise width of the test section. The resulting time scale is given by  $t_s=D/U_o$ . The major implication of the Stokes number is that particles with a small Stokes number ( $St\ll 1$ ) are found to be in near velocity equilibrium with the surrounding carrier fluid, making them extremely or totally responsive to fluid velocity fluctuations. In fact, this feature has been exploited in LDV/PIV/LDA, where particles are used as tracers to follow the flow field, including the fine mist of 5% sugar solution from the atomizer used in our study, to measure the gas phase velocities. However, particles with a larger Stokes number ( $St\gg 1$ ) are found to be no longer in equilibrium with the surrounding fluid phase as they are

unresponsive to fluid velocity fluctuations and they will pass unaffected through eddies and other flow structures, with a possibility to modify them. Based on the above definition, the Stokes number for the particles considered in this study is 3.25.

From the Stokes number definition, one can deduce that the particles used in our experiments are no longer in equilibrium with the surrounding gas. They behave somewhat independently of the gas phase in both streamwise and transverse velocity directions. Depending on the section within the bend they may move faster than the gas phase or may lag behind the gas phase. Depending on the movement of the particles they setup slip velocities. These slip velocities in turn give rise to particle drag. The gas phase which is embodied with these particles, lose some of their velocity trying to overcome this drag. This helps to explain why the unclean gas in majority of the test section lag behind the clean gas which has no particles in it.

## CONCLUSION

Simultaneous measurements of both the gas and solid phases in a dilute turbulent two-phase flow system inside a 90° duct bend have been successfully investigated. Size discrimination technique using a PDA was used to separate the gas from the particulate phase. Streamwise and transverse velocities of clean gas (without the particles) and unclean gas (with particles) were compared along various sections of the bend and the vertical duct past the bend. It is concluded that the mean velocities of the unclean gas lagged behind the clean gas and this was mainly due to the effect of particle drag or the part of energy spent by the gas phase moving the particles within its flow field. The current experimental data can be used to further enhance CFD models, to aid better prediction near the inner wall of the bend by establishing an effective two-way coupling between the gas and the particulate phases.

## ACKNOWLEDGEMENT

The authors would like to thank Dr Chris Solnordal for his editorial skills in improving the quality of the published manuscript.

## REFERENCES

- BILIRGEN, H. and LEVY, E.K., (2001), "Mixing and dispersion of particle ropes in lean phase pneumatic conveying", *Powder Tech*, 119, 134-152.
- DURST, F. and ZARE, M., (1975), "Laser-doppler measurements in two-phase flows", *Proceedings of the LDA-Symposium Copenhagen*, 403-429
- HUBER, N. and SOMMERFELD, M., (1994), "Characterization of the cross-sectional particle concentration distribution in pneumatic conveying systems". *Powder Tech*, 79, 191-210.
- HUMPHERY, J.A.C., WHITELAW, J.H. and YEE, G., (1981), "Turbulent flow in a square duct with strong curvature", *J.Fluid Mech.* 103, 443-463.
- KLIAFAS, Y. and HOLT, M., (1987), "LDV measurements of a turbulent air-solid two phase flow in a 90° Bend", *Exp. Fluids*, 5, 73-85.
- KUAN, B., YANG, W. and SCHWARZ, M.P., (2007), "Dilute gas-solid two-phase flows in a curved 90° duct

bend: CFD simulation with experimental validation”, *Chem Engg. Sc*, 62, 2068-2088.

MOHANARANGAM, K., TIAN, Z. F. and TU, J. Y., (2007), “Numerical simulation of turbulent gas–solid particle flow in a 90° bend: Eulerian-Eulerian approach”, *Comp & Chem Engg*, 41, 561–571.

TU, J. Y. and FLETCHER, C. A. J., (1995), “Numerical computation of turbulent gas–solid particle flow in a 90° bend”, *AIChE Journal*, 41, 2187–2197.

YANG, W. and KUAN, B., (2006), “Experimental investigation of dilute turbulent particulate flow inside a curved 90° bend”, *Chem Engg. Sc*, 61, 3593-3601.

YILMAZ, A. and LEVY, E.K., (2001), “Mixing and dispersion of particle ropes in lean phase pneumatic conveying”. *Powder Tech*, 114, 168-185.

YILMAZ, A. and LEVY, E.K., (1998), “Roping phenomena in pulverized coal conveying lines”. *Powder Tech*, 95, 43-48.

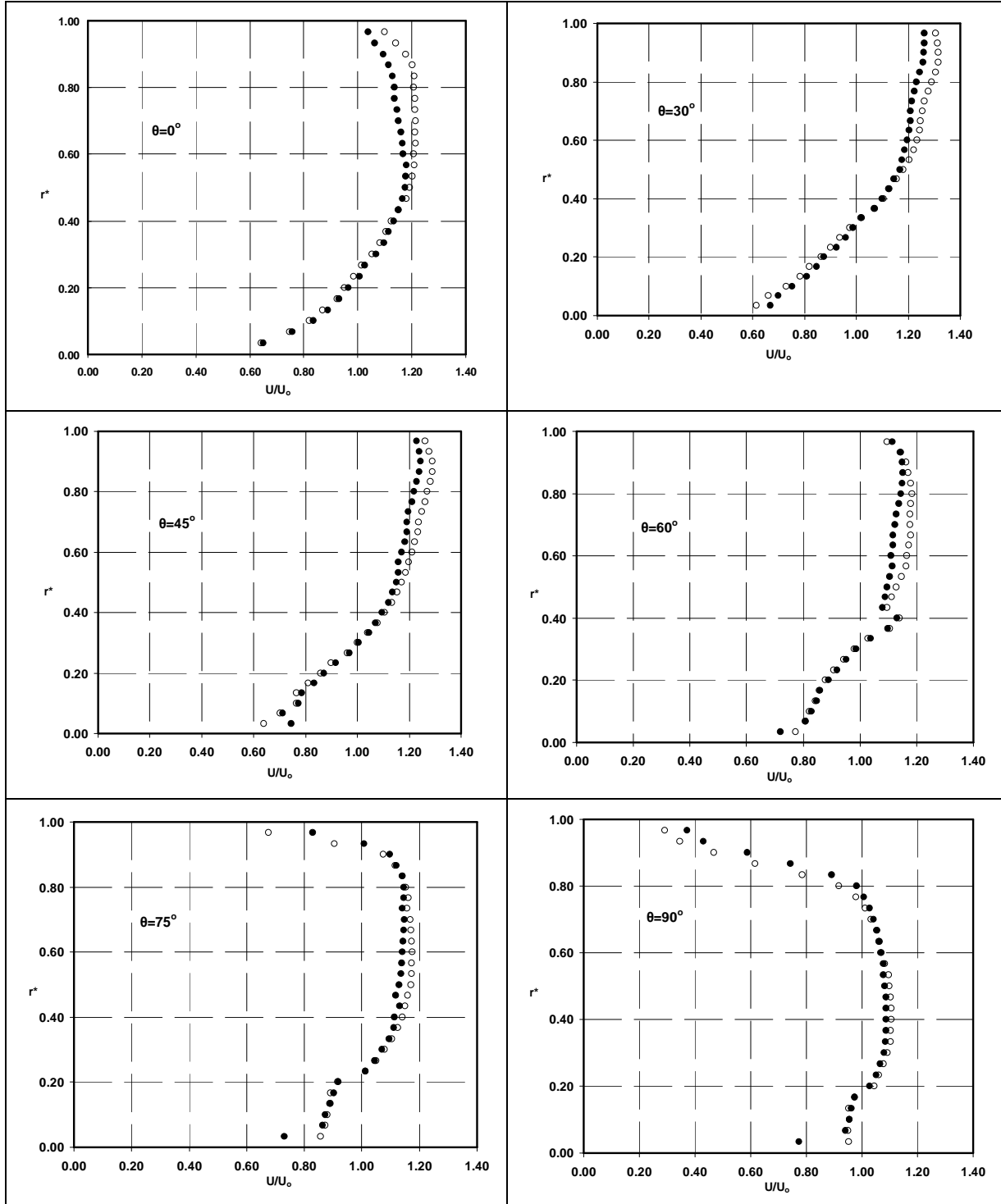
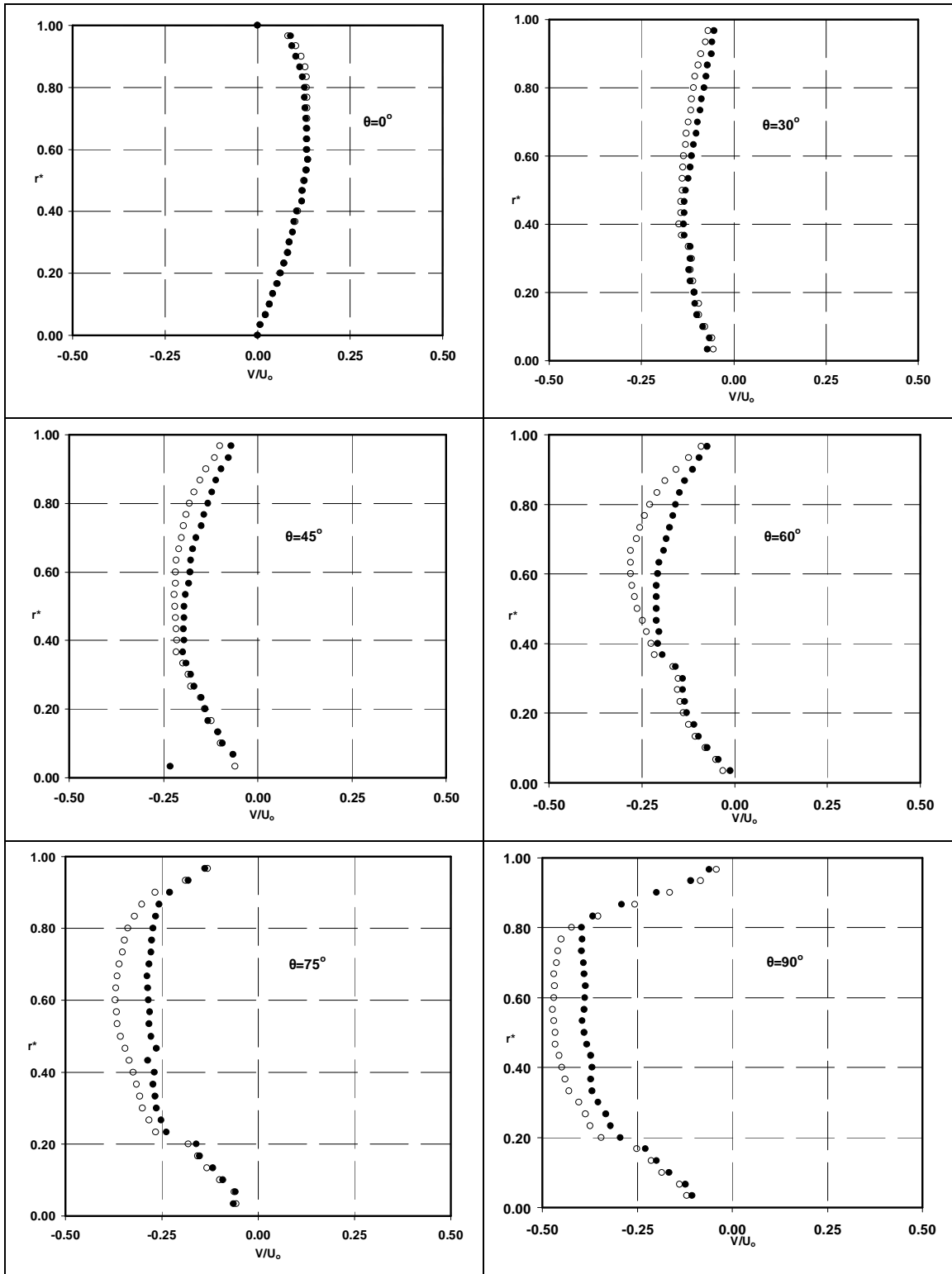
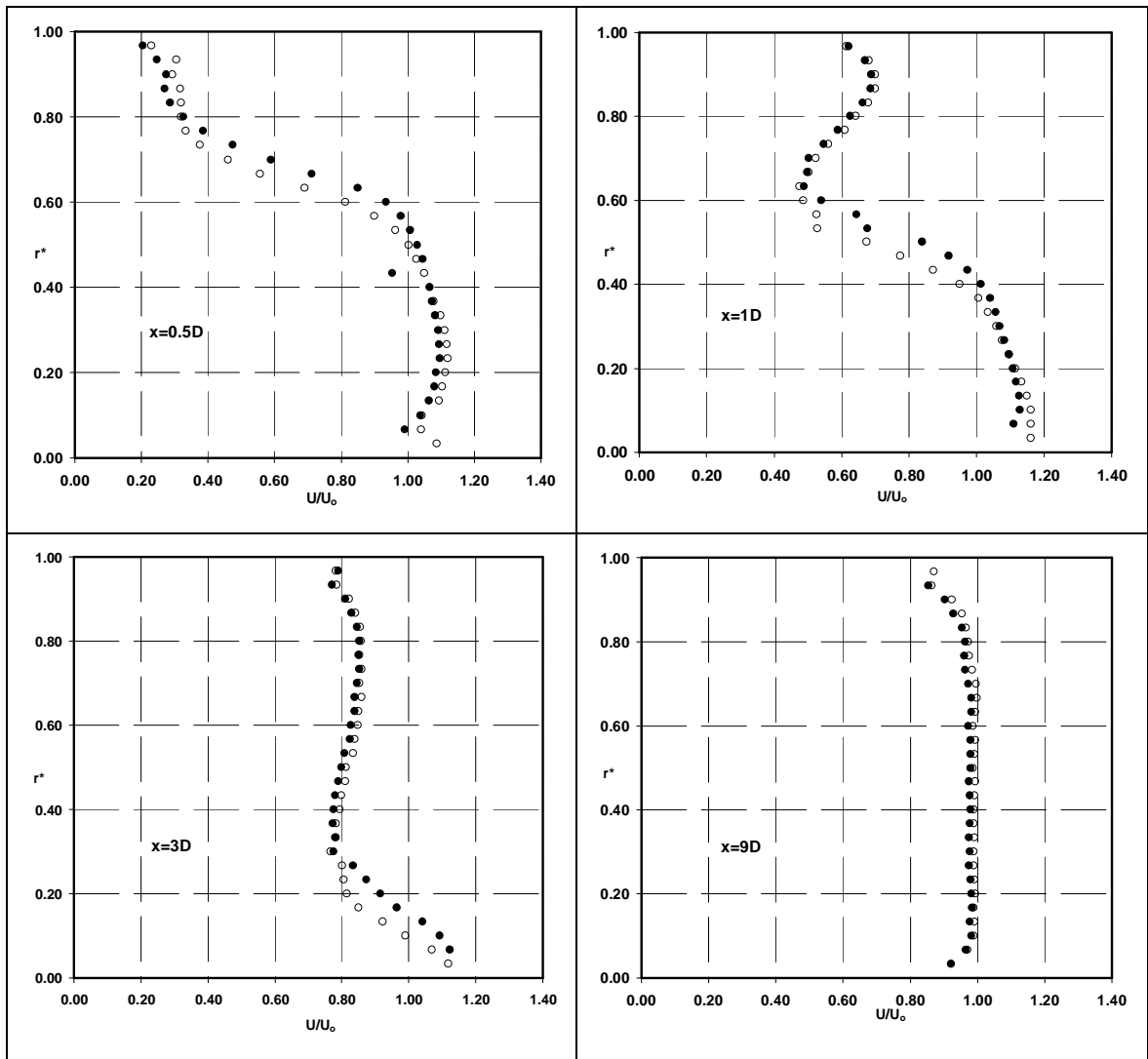


**Figure 2.** Mean streamwise velocities of gas with and without particles, six traverses along the bend



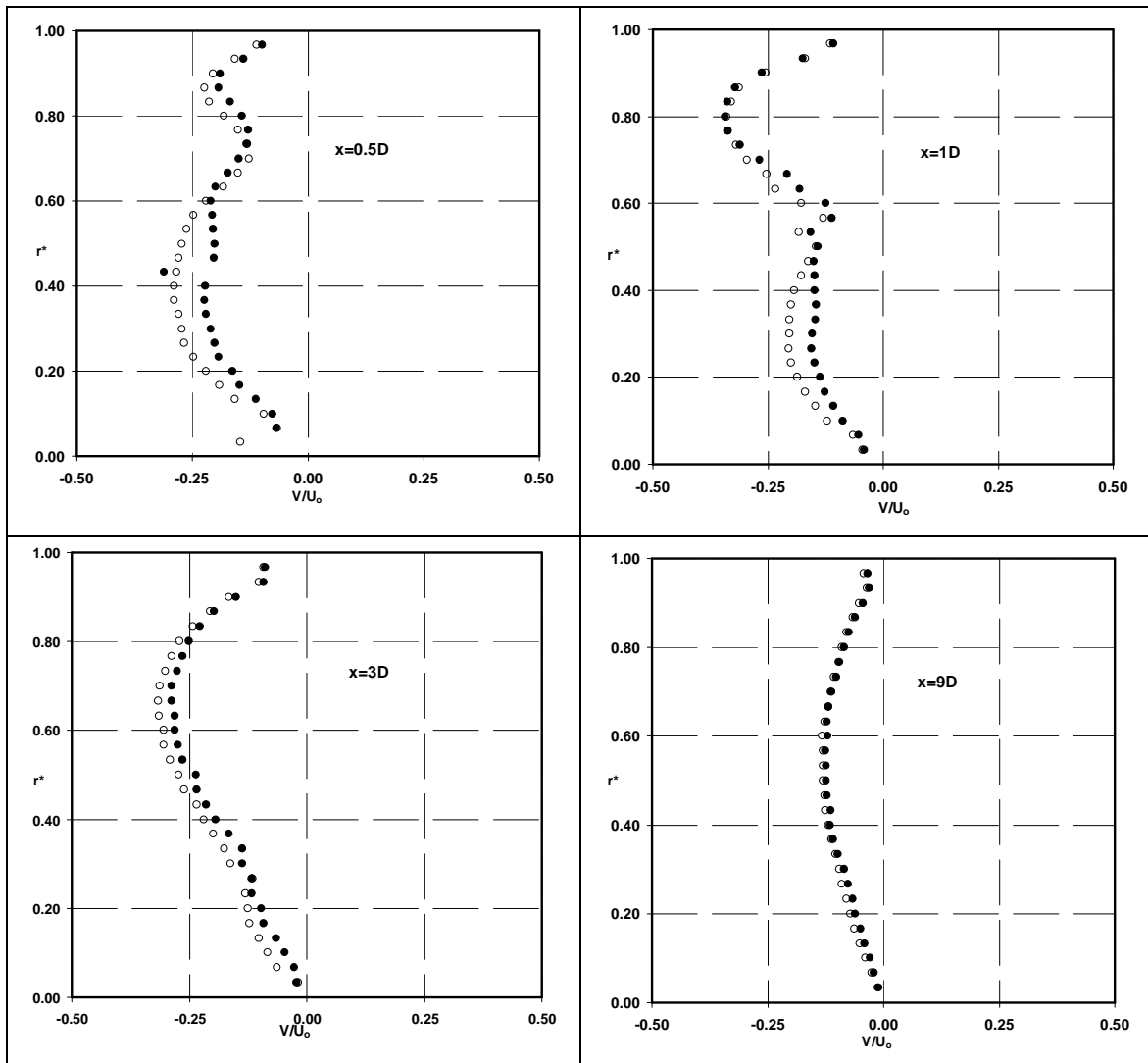
○ Clean gas ● Unclean gas

**Figure 3.** Mean transverse velocities of gas with and without particles, six traverses along the bend



○ Clean gas ● Unclean gas

**Figure 4.** Mean streamwise velocities of gas with and without particles. Four locations along the downstream vertical duct



○ Clean gas ● Unclean gas

**Figure 5.** Mean transverse velocities of gas with and without particles. Four locations along the downstream vertical duct